PROF. GIANFRANCO ALPINI (Orcid ID : 0000-0002-6658-3021)
DR. ATHANASIOS PAPAKYRIAKOU (Orcid ID : 0000-0003-3931-6232)
PROF. GEORGIOS GIAMAS (Orcid ID : 0000-0002-4417-2707)
DR. SALVATORE PAPA (Orcid ID : 0000-0002-8369-6538)

Phosphorylation and stabilization of PIN1 by JNK promote intrahepatic cholangiocarcinoma growth

Alessio Lepore[1,#], Pui Man Choy[2,#], Nathan CW Lee[1], Maria Annunziata Carella[3], Rosy Favicchio[4], Marco A Briones-Orta[2,5], Shannon S Glaser[6], Gianfranco Alpini[7], Clive D'Santos[8], Reuben M Tooze[1], Mihaela Lorger,[1] Wing-Kin Syn[2,9,10,11], Athanasios Papakyriakou[12], Georgios Giamas[13], Concetta Bubici[3,§] and Salvatore Papa[1,2,§,*]

1. Leeds Institute of Medical Research at St James', Faculty of Medicine and Health, University of Leeds, St. James' University Hospital, Leeds, UK.
2. Institute of Hepatology, Foundation for Liver Research and Birkbeck, University of London, London, UK.
3. Centre for Genome Engineering and Maintenance, Department of Life Sciences, College of Health, Medicine and Life Sciences, Brunel University London, Uxbridge, UK.
4. Department of Surgery and Cancer, Imperial College, London, UK.
5. Department of Infectious Disease, Imperial College, London, UK.
6. Department of Medical Physiology, Texas A&M University, Bryan, TX.
7. Richard L. Roudebush VA Medical Center and Indiana University, Gastroenterology, Medicine, Indianapolis, IN, USA.
8. Cancer Research UK Cambridge Institute, University of Cambridge, Robinson Way, Cambridge, UK.
9. Section of Gastroenterology, Ralph H Johnson Veterans Affairs Medical Center, Charleston, USA.
10. Division of Gastroenterology and Hepatology, Department of Medicine, Medical University of South Carolina, Charleston, SC USA.

This article has been accepted for publication and undergone full peer review but has not been through the copyediting, typesetting, pagination and proofreading process, which may lead to differences between this version and the Version of Record. Please cite this article as doi: 10.1002/HEP.31983

11. Department of Physiology, Faculty of Medicine and Nursing, University of Basque Country UPV/EHU, Leioa, Spain.
12. Institute of Biosciences and Applications, National Centre for Scientific Research "Demokritos", Athens, Greece.
13. Department of Biochemistry and Biomedicine, School of Life Sciences, University of Sussex, Brighton, UK.

# These authors contributed equally to this work.
§ These authors contributed equally and jointly supervised this work.
*** Correspondence should be addressed to**:
Dr. Salvatore Papa; St James' University Hospital, Beckett Street, Wellcome Trust Brenner Building, 6.14, Leeds LS9 7TF, UK; Email: s.papa@leeds.ac.uk

Key words: cancer, post-translational modification, oncogenes, ubiquitin, bile duct cancer

Competing interests

The authors declare that they have no competing interests

Funding

This study was primarily supported by research grants from 250 Great Minds University Academic Fellowship University of Leeds, AMMF Cholangiocarcinoma Charity, Foundation for Liver Research (to SP) and Brunel Research Initiative & Enterprise Fund (LBL348) Brunel University of London (to CB); and in part by research grants from Blood Cancer UK (17014) (to SP, CB and RMT), Rosetrees Trust (M894) and Guts UK (DGO2019_02) (to SP and CB)

Authors Contributions

AL, PMC, NCL, MAC, CB and SP performed the majority of the experiments. RF, GG and ML helped with animal studies and data analyses. MAB-O performed quantitative pcr. SSG and GA provided essential reagents and helped with data analyses. CD'S performed mass spectrometry analyses. AP performed the computational modelling and interpretation. RMT and W-K S helped with data analyses and interpretation. CB and SP are both senior authors, conceived idea, chiefly carried out data analysis and interpretation, coordinate the study, obtained research funding and wrote the manuscript, which was commented by all the authors.

Acknowledgements

We thank Ulf Klein (University of Leeds) for insightful comments to the manuscript. We thank Michael B. Yaffe (MIT Center for Precision Cancer Medicine) for the GST-PIN1 plasmid; J. Zhang (Duke University) for the JNK1^{CA} and JNK2^{CA}; G. Franzoso (Imperial College London) for the c-Jun and shRNA lentiviral vectors; and D. Trono (Ecole Polytechnique Federale de Lausanne, Switzerland) for the pWPI lentiviral vector; D. Guardavaccaro (University of Verona) for the pWC7-His-Myc-Ubiquitin-WT, pCMV-His-HA-Ubiquitin-WT and pWC7-His-Myc-Ubiquitin K0. We thank L. Jary, D. Evans and J Bilton (University of Leeds) for technical assistance.

List of abbreviations

ICC: Intrahepatic cholangiocarcinoma; JNK: c-Jun N-terminal kinase; JNK1^{CA}: JNK1 constitutive active; JNK2^{CA}: JNK2 constitutive active; MAPK: mitogen-activated protein kinase; PIN1: Protein Interacting with NIMA-1; PPIase: peptidyl-prolyl cis-trans isomerase; PDAC: pancreatic ductal adenocarcinoma; ATRA: all-trans retinoic acid; APL: acute promyelocytic leukaemia; BrdU: Bromodeoxyuridine; Phos-Tag: phosphate-affinity gel electrophoresis; GST: glutathione S-transferase; ATP: Adenosine triphosphate; IPTG: Isopropyl-β-D-thiogalactoside; PD: pulldown; KA: kinase assay; rPIN1: shRNA-resistant PIN1; shRNA: short hairpin RNA; EV: empty vector; NS: non-specific; RMSF: root-mean-square fluctuations; MD: molecular dynamics; SASA: solvent-accessible surface area; CHX: cycloheximide; WB: western blot; PCR: polymerase chain reaction.

ABSTRACT

Background and Aims

Intrahepatic cholangiocarcinoma (ICC) is a highly aggressive type of liver cancer in urgent need of treatment options. Aberrant activation of c-Jun N-terminal kinase (JNK) pathway is a key feature in ICC and an attractive candidate target for its treatment. However, the mechanisms by which constitutive JNK activation promotes ICC growth, and thus the key downstream effectors of this pathway remain unknown for their applicability as therapeutic targets. Our aim was to obtain a better mechanistic understanding of the role of JNK signalling in ICC that could open new therapeutic opportunities.

Approach and Results

Using loss- and gain-of-function studies *in vitro* and *in vivo*, we show that activation of the JNK pathway promotes ICC cell proliferation by affecting the protein stability of Peptidyl-prolyl cis-trans isomerase NIMA-interacting 1 (PIN1), a key driver of tumorigenesis. PIN1 is highly expressed in ICC primary tumours, and its expression positively correlates with active JNK. Mechanistically, the JNK kinases directly bind to and phosphorylate PIN1 at Ser115, and this phosphorylation prevents PIN1 mono-ubiquitination at Lys117 and its proteasomal degradation. Moreover, pharmacological inhibition of PIN1 via a*ll-trans* retinoic acid (ATRA), an FDA-approved drug, impairs the growth of both cultured and xenografted ICC cells.

Conclusions

Our findings implicate the JNK-PIN1 regulatory axis as a functionally important determinant for ICC growth, and provide a rationale for therapeutic targeting of JNK activation via PIN1 inhibition.

Intrahepatic cholangiocarcinoma (ICC) is a tumour of the bile ducts within the liver that mainly arises from an uncontrolled proliferation of transformed cholangiocytes. With a global increasing incidence and mortality rates, ICC represents the second most frequent primary liver tumour after hepatocellular carcinoma (1-3). Currently, there are no curative chemotherapies for ICC, and efforts to develop molecular-targeted therapies have been limited due to the lack of a detailed understanding of the molecular mechanisms underlying the disease (2).

ICC usually develops in the context of both chronic inflammation of the biliary tract and liver injury that foster the accumulation of genetic mutations in proto-oncogenes and tumour suppressors, such as KRAS and p53, which in turn lead to the constitutive activation of signalling pathways involved in cell proliferation (4-7). One of the major signalling pathways that are activated by mutant KRAS in ICC models is the JNK signalling (8), a member of the mitogen-activated protein kinase (MAPK) family (9-11). Activation of JNK signalling facilitates the development of ICC by promoting the hyperproliferation of transformed bile duct cells (8). Although the pharmacologic inhibition of the JNK kinase activity impairs the development of ICC in several mouse models of liver injury (8), active JNK is a challenging protein to target, due to its physiological and cell-type-specific functions in the liver (12-15). Therefore, we sought to obtain a better understanding of the mechanisms by which active JNK signalling promotes ICC, because the identification of the major downstream effectors of the JNK/MAPK pathway could lead to the development of much needed molecular-targeted therapeutics.

A key downstream effector of the oncogenic KRAS signal is PIN1, an evolutionarily conserved peptidyl-prolyl *cis-trans* isomerase (PPIase). PIN1 catalyses the *cis-trans* isomerization of peptidyl-prolyl bonds in phosphorylated Ser/Thr-Pro motifs of the target proteins (16-21). Through its PPIase activity, PIN1 affects the function of a large and diverse array of phosphorylated target proteins, including oncoproteins and tumour suppressors (18-24). PIN1 is frequently highly expressed in human cancers, and its expression correlates with poor patient prognosis (20,24). For instance, PIN1 is overexpressed in invasive ductal carcinoma breast cancer, and cooperates with activated JNK and oncogenic RAS in promoting deregulated cell proliferation through increasing the expression of the cell cycle regulator cyclin D1 (16,17,24). PIN1 also cooperates with oncogenic KRAS in driving cellular transformation in pancreatic ductal adenocarcinoma (PDAC) and is required for PDAC cell viability (21). Given that ICC is driven by mutant KRAS and active JNK (4,5,8), and that a proportion of invasive ductal carcinoma breast cancer and PDAC share an inflammatory origin with ICC (8,25,26), an interesting question is whether PIN1 plays a role in ICC. Yet, since genetic and/or genomic studies to date have rarely found mutations and

amplifications of the PIN1 gene (24), the molecular mechanisms underlying PIN1 overexpression need to be understood at cell signalling level.

Here we demonstrate that the constitutive activation of JNK leads to elevated levels of PIN1 expression thus promoting ICC cell proliferation. We show that JNK proteins directly interact with and phosphorylate PIN1 at Ser115. The phosphorylation of PIN1 at this specific residue directly causes the increase in intracellular PIN1 levels by preventing its mono-ubiquitination at Lys117 and, consequently, inhibiting its proteasomal degradation. We also show the potential application of PIN1 inhibition using ATRA (27) for ICC therapy.

MATERIALS AND METHODS

Tissue microarrays (TMAs) and immunohistochemistry (IHC)

Formalin fixed paraffin-embedded human intrahepatic cholangiocarcinoma (ICC) used in Tissue microarrays were purchased from Pantomics (tissue block LVC1261), consisting of 42 cases, 126 cores, one normal adjacent nontumor liver tissue core paired with two tumour tissue cores from each patient. IHC staining of sequential sections was carried out using a two-step protocol. After antigen retrieval, each TMAs slide, consisting of serial tissue cuts was incubated with validated anti-human PIN1 antibody (1:50; H123, Santa Cruz Biotechnology) (28) and anti-human phospho(p)-JNK (1:50; 9251, Cell Signaling Technology) (29,30). The quantification of PIN1 and p-JNK staining was evaluated by choosing randomly five non-overlapping fields at 40X for each core and quantified by counting the number of PIN1(+) or p-JNK(+) biliary epithelial cells/field and dividing by the total number of biliary epithelial cells/field.

Xenograft tumour models

For xenograft experiments, $3x10^6$ CCLP1 parental or sh-NS-, shJNK1/2-, shPIN1-expressing cells were injected subcutaneously into dorsal regions of 8-week-old female NOD/SCID (strain 394, Charles River) immunodeficient mice. Body weight and tumour sizes were recorded overtime by a calliper and tumour volumes were calculated using the formula: $LxW^2x0.52$, where L and W represent length and width, respectively. For ATRA treatment, two weeks later mice injected with CCLP1 parental cells were randomly selected to receive ATRA or control (placebo) treatment using time (over 21 days)-release drug pellets. For implantation, placebo or 10 mg of ATRA-releasing pellets (Innovative Research of America) were implanted subcutaneously in the flank of tumour-bearing NOD/SCID mice. At sacrifice, the tumours were recovered, photographed and the

wet weight of each tumour was recorded. Each tumour was snap frozen for further analysis. All experiments were carried out with approval from UK Home Office Authority (PPL70/8448; PEA0105B1) (31).

Statistical analysis

Statistical analyses were performed with Prism 8.0 (GraphPad Software). For two pairwise comparisons two-tailed Student's t tests were performed. One-way ANOVA was performed to determine differences between each group when more than two conditions were present. A two-way ANOVA test was used to test the effect of two independent variables on a dependent variable. Error bars represent standard error of the mean (s.e.m). A value of $P<0.05$ was considered significant.

Additional methods are provided as supplementary material.

RESULTS

JNK activity correlates with PIN1 expression and regulates its protein levels in cholangiocarcinoma

As RAS mutations are a key event in cholangiocarcinogenesis (4-7), and both PIN1 and JNK activation were previously identified as downstream targets of oncogenic RAS (9-11,16,20), we investigated a possible relationship between PIN1 and JNK signalling in ICC. First, we analysed the expression levels of PIN1 and phospho-JNK (p-JNK; a proxy for active JNK) in consecutive sections of ICC tissue microarray by immunohistochemistry using antibodies of anti-PIN1 (28) or anti-p-JNK (29), which detect phosphorylated JNK1 and JNK2, two major JNK kinases. We found that, compared with adjacent nontumour biliary cells, an increased percentage of ICC epithelial cells expressed PIN1 (18.64 *vs*. 41.25) and p-JNK (6.19 *vs.* 20.13), the levels of which positively correlated each other (**Fig. 1A, B; Supplementary Fig. S1A**). Using WB, we then evaluated the expression of PIN1 and p-JNK in ICC-derived cell lines (CCLP1, HuCCT1 and SG231) and observed higher levels of both PIN1 and p-JNK in all three ICC cell lines when compared to primary normal intrahepatic biliary epithelial cells (HIBEpiC) (**Fig. 1C).** Moreover, analysis of JNK activation by *in-vitro* kinase assays (K.A.) showed considerable increase of the kinase activities of JNK1 and JNK2 in ICC cells compared with nontumoral immortalized human H69 cholangiocytes (32), while the overall PIN1 protein levels were similar in ICC and H69 cells (**Fig. 1D),** suggesting a potential JNK-PIN1 pathway that is specific to ICC.

Next, we knocked down the expression of JNK proteins in ICC cells using short-hairpin (sh)RNA lentiviruses targeting both JNK1 and JNK2 (shJNK1/2) and analysed PIN1 expression levels. As controls, we used lentiviruses expressing nonspecific shRNA (shNS) (29). Efficient knockdown was verified by WB (**Fig. 1E**). Knockdown of JNK1/2 resulted in a marked reduction of PIN1 protein levels (**Fig. 1E**) with no significant effect on PIN1 mRNA levels (**Fig. 1F**), suggesting that JNK proteins regulate PIN1 at post-transcriptional level. Similar results were obtained in ICC cells depleted of either JNK1 or JNK2 (**Supplementary Fig. S1B, C**). Intriguingly, reduced PIN1 protein levels were not observed in JNK1/2-silenced H69 cells (**Fig. 1E**). This indicates that the effect of JNK on PIN1 expression is specific to ICC cells, in which JNK is constitutively active (see **Fig. 1C, D**). Indeed, a decrease in PIN1 protein levels was observed when we treated ICC cells with the JNK inhibitor SP600125 (33) (**Fig. 1G**), which specifically blocked phosphorylation/activity of JNK1/2 without affecting phosphorylation/activity levels of other related MAPK proteins (ERK and p38) (9). Remarkably, no significant differences in phosphorylation/activity levels of JNK were observed when we knocked down PIN1 expression in ICC cells using PIN1 shRNA (shPIN1) (**Supplementary Fig. S1D**), which is consistent with the hypothesis that JNK proteins function upstream of PIN1. Moreover, WB of lysates from CCLP1 cells infected with a lentivirus expressing a constitutively active form of JNK1 ($JNK1^{CA}$) (30) revealed that expression levels of endogenous PIN1 were increased compared to control cells (**Fig. 1H**), suggesting a role for JNK activity in up-regulating PIN1 protein levels.

PIN1 functionally mimics JNK activation in cholangiocarcinoma cells

Because JNK activity positively regulates PIN1 protein levels (see **Fig. 1E, G, H; Supplementary Fig. S1B)** and its inhibition impairs ICC cell proliferation (8), we investigated whether this was the case for PIN1. Compared with control silencing, knockdown of PIN1 significantly attenuated the growth rate and reduced colony-forming ability of ICC cells to the same extent as JNK1/2 knockdown (**Fig. 2A-D; Supplementary Fig. S2A-C**). The growth defect of PIN1-depleted cells was specific to the lack of PIN1, as reconstituted expression of shRNA-resistant wild-type PIN1 (rPIN1 WT) in these cells reversed this defect (**Supplementary Fig. S2D**). The effects of knockdown of either PIN1 or JNK1/2 were also confirmed by decreased cell mass accumulation (**Supplementary Fig. S2E-G**). Notably, depletion of either PIN1 or JNK1/2 had no effect on the growth rate or cell mass accumulation of H69 cells (**Fig. 2A, B; Supplementary Fig. S2E-G**). Furthermore, we observed a significant reduction of BrdU incorporation in PIN1 knockdown cells with a concomitant decrease in the levels of various cell-cycle regulators (**Supplementary Fig. S2H, I**), indicating that PIN1 depletion attenuates ICC cell proliferation. These reductions occurred

in the absence of any significant induction of apoptosis as determined by measurement of the percentage of the sub-G1 population and caspases cleavage (**Supplementary Fig. S2J, K**). Similar results were observed in JNK1/2 knockdown cells (**Supplementary Fig. S2L-O**). Moreover, when subcutaneously injected into NOD/SCID immunodeficient mice, CCLP1 cells with PIN1 or JNK1/2 knockdown gave rise to smaller tumours compared with those of control silencing, as revealed by measuring tumour mass and weight (**Fig. 2E-H**). In contrast to the effects induced by PIN1 depletion, ectopic expression of PIN1 led to a significant increase in growth rate and colony formation of ICC cells (**Fig. 2I, J**). These effects faithfully mimicked those of $JNK1^{CA}$ overexpression (**Fig. 2K, L**). Together, these results indicate that PIN1 promotes ICC cell proliferation both *in vitro* and *in vivo* to a similar degree as JNK activation and suggest that JNK inhibition may impair ICC cell proliferation by lowering PIN1 levels.

JNK inhibition decreases PIN1 levels via promoting its monoubiquitin-proteasome degradation

The observation that JNK1/2 knockdown results in a decrease in PIN1 protein levels without affecting the levels of its mRNA (**Fig. 1E, F; Supplementary Fig. S1B, C**) led us to examine whether JNK1/2 regulated PIN1 protein stability. For this purpose, we evaluated the half-life of PIN1 by performing pulse-chase assays in the presence of cycloheximide (CHX), which blocks protein synthesis. Depletion of JNK1/2 or chemical inhibition of JNK activity resulted in a decrease in the half-life of endogenous PIN1 in CCLP1 cells (**Fig. 3A, B**). Conversely, co-expression of $JNK1^{CA}$ but not a catalytically non-active JNK1 protein resulted in an increase of the half-life of PIN1 in HEK293T cells (**Supplementary Fig. S3A, B**). These findings indicate that active JNK1/2 upregulate PIN1 levels by enhancing its protein stability.

As PIN1 has been reported to be degraded via the ubiquitin-proteasome system (34-36), we examined whether JNK proteins elicit their effects on PIN1 stability via inactivation of the ubiquitin-proteasome system (37). Treatment of JNK1/2-depleted ICC cells with the proteasome inhibitor MG132 was sufficient to completely revert the decrease in PIN1 protein levels in these cells (**Fig. 3C**), indicating that proteasome mediates the effects of JNK1/2 depletion on PIN1 levels. Similar results were obtained when we added MG132 to ICC cells pre-treated with SP600125 to inhibit JNK activity (**Fig. 3D**). We then asked whether JNK could affect PIN1 ubiquitination, a key post-translational modification required for proteasomal degradation. FLAG-tagged PIN1 and His-tagged ubiquitin were co-expressed in HEK293T cells with or without HA-tagged $JNK1^{CA}$, and the ubiquitination status of PIN1 was assessed by combined Ni-NTA pull-down (PD) and WB analyses. Expression of $JNK1^{CA}$ prevented the appearance of a single band corresponding in molecular weight to the monoubiquitinated form of PIN1 (**Supplementary Fig.**

S3C). Such an effect was also confirmed by co-immunoprecipitation (IP) analyses (**Supplementary Fig. S3D**). Similar results were obtained when a mutant form of ubiquitin (UbK0), which allows only monoubiquitination due to the lack of lysine residues (38), was used instead of wild-type ubiquitin (**Supplementary Fig. S3E**). This confirms that PIN1 is subject to monoubiquitination, which is inhibited by $JNK1^{CA}$ expression. Such inhibition was not observed when we co-expressed the catalytically non-active JNK1 protein (**Supplementary Fig. S3F**), suggesting that JNK kinase activity is required for preventing PIN1 mono-ubiquitination. Importantly, the inhibitory effect of JNK on PIN1 mono-ubiquitination was confirmed in ICC cells as accumulation of endogenous monoubiquitinated PIN1 was observed in JNK1/2-depleted CCLP1 cells (**Fig. 3E**). Thus, the constitutive activation of JNK in ICC cells leads to high levels of PIN1 by preventing its mono-ubiquitination and degradation.

Active JNK proteins interact with and phosphorylate PIN1 at Ser115

To gain insight into the mechanism by which JNK proteins stabilize PIN1, we co-expressed HA-tagged PIN1 in HEK293T cells with FLAG-tagged $JNK1^{CA}$, FLAG-tagged $JNK2^{CA}$ or empty vector, and investigated protein associations by combined IP and WB analyses. Both FLAG-tagged $JNK1^{CA}$ and FLAG-tagged $JNK2^{CA}$ specifically bound to HA-PIN1 (**Supplementary Fig. S4A**). Furthermore, *in-vitro* kinase assays revealed that both active JNK1 and JNK2 efficiently phosphorylated recombinant GST-fused PIN1, but not GST alone (**Fig. 4A**). As JNK1 and JNK2 shared common function with respect to their interaction with PIN1 and its phosphorylation, we focused our attention on JNK1 in further analyses. First, the interaction between PIN1 and active JNK1 was confirmed at the endogenous levels. Anti-active-JNK1 antibodies (29,30) co-immunoprecipitated PIN1 from parental cells, but not from ICC cells depleted of PIN1 (**Fig. 4B**; WB:PIN1). JNK1 was immunoprecipitated at comparable levels in both parental cells and PIN1-depleted cells and was not co-precipitated by isotype-matched control antibodies (**Fig. 4B**; WB:JNK1). We then verified that PIN1 was phosphorylated by JNK1 in *in-vivo* cells. PIN1 co-expressed with $JNK1^{CA}$, but not with the catalytically non-active JNK1 protein, was highly phosphorylated in HEK293T cells as shown by a marked band shift of PIN1 on Phos-tag polyacrylamide gel electrophoresis (39). This shifted band disappeared when cell lysates were treated with the calf intestinal alkaline phosphatase (CIP) (**Supplementary Fig. S4B**), confirming that the shifted band of PIN1 was a consequence of phosphorylation by active JNK1. Importantly, phosphorylation of endogenous PIN1 by JNK was confirmed in ICC cells, as the PIN1 shifted band disappeared in JNK1/2-depleted or SP600125-treated CCLP1 cells on Phos-tag immunoblots (**Fig. 4C**), indicating that PIN1 is indeed phosphorylated by JNK proteins in ICC cells.

To test whether JNK could directly phosphorylate PIN1, we performed *in-vitro* kinase assays and found that recombinant active JNK1 efficiently phosphorylated purified His-PIN1 (**Fig. 4D**). Accordingly, *in-vitro* pull-down analyses revealed direct interaction between active JNK1 and PIN1 (**Fig. 4E**). Altogether, these data indicate that PIN1 is a direct substrate of JNK1 kinase. In support of this notion, a single phosphorylation site (Ser115) was detected in PIN1 by mass spectrometry (**Supplementary Fig. S4C-F**). Sequence alignment analysis of PIN1 revealed that Ser115 is conserved among different species and located within the consensus phosphorylation motif for JNKs (^{115}SA^{116}) (40) (**Supplementary Fig. S4G**). To confirm Ser115 as the specific JNK1 phosphorylation site on PIN1, a non-phosphorylatable alanine PIN1 mutant (S115A) was generated and used as a substrate for JNK1 in kinase assays. As controls, we individually mutated Ser114, a nearby JNK consensus phosphorylation site (^{114}SS^{115}), and Ser138, a residue known to be phosphorylated by the JNK-related kinase mixed-lineage kinase 3 (MLK3) (41), into alanines (S114A and S138A). PIN1-S115A mutant, but not wild-type PIN1, PIN1-S114A or PIN1-S138A mutant was resistant to phosphorylation by JNK1 *in vitro* (**Fig. 4F**). This result was confirmed in ICC cells expressing endogenous active JNK and in HEK293T cells expressing exogenous constitutively active JNK1 by Phos-tag immunoblots (**Fig. 4G; Supplementary Fig. S4H**). Taken together, these results indicate that JNK1 directly phosphorylates PIN1 at Ser115 both *in-vitro* and in *in-vivo* cells.

Phosphorylation of PIN1 at Ser115 prevents its mono-ubiquitination and degradation

To directly test the role of Ser115 phosphorylation in the control of PIN1 protein stability, we generated CCLP1 cells stably expressing FLAG-PIN1-WT, -S114A, -S115A or -S138A mutant and assessed the half-life of PIN1 mutant proteins in these cells, which have endogenous active JNK (see **Fig. 1C, D**). Endogenous active JNK failed to prolong the half-life of the PIN1-S115A mutant, but not of PIN1-WT, PIN1-S114A or PIN1-S138A mutant (**Fig. 5A**), implying that phosphorylation of PIN1 at Ser115 is required for PIN1 protein stability. Accordingly, PIN1-S115A mutant was heavily monoubiquitinated in CCLP1 cells, whereas wild-type PIN1 was resistant to monoubiquitination (**Fig. 5B**), indicating that PIN1-S115A mutant is targeted for degradation. Similar results were observed in HEK293T cells ectopically expressing JNK1^{CA} (**Supplementary Fig. S5A, B;** see also **Supplementary Fig. S3C**). Collectively, these data indicate that JNK-mediated PIN1 phosphorylation at Ser115 is essential for PIN1 protein stability. We next sought to identify the lysine residue on PIN1 that is targeted for mono-ubiquitination. As the vast majority of protein ubiquitination sites tend to be exposed to the solvent (42,43), we calculated the solvent-accessible surface area (SASA) of the ten lysine residues (K6, K13, K46, K63, K77, K82, K95, K97, K117 and K132) in the high-resolution X-ray crystal structure of PIN1 (PDB ID:1PIN) (44).

Lys117 emerged as the lysine residue with the highest solvent-accessibility (**Fig. 5C; Supplementary Table S1**), suggesting that K117 is a highly exposed residue thus may serve as the PIN1 ubiquitination site. Indeed, mutation of Lys117 to arginine (K117R) abolished mono-ubiquitination of PIN1 (**Fig. 5D; Supplementary Fig. S5C**), and subsequently resulted in an increase of PIN1 half-life in *in-vivo* cells (**Fig. 5E; Supplementary Fig. S5D**). Although we cannot completely rule out by site-directed mutagenesis that other lysine residues within PIN1 could be targets for mono-ubiquitination, mutating Lys46, which has the second highest solvent-accessibility, did not abrogate the ubiquitination of PIN1 (**Supplementary Fig. S5C**). These results indicate that, most likely, Lys117 residue on PIN1 is the major site subjected to mono-ubiquitination needed for its degradation.

To gain insights into the structural basis of Ser115 phosphorylation-mediated inhibition of PIN1 mono-ubiquitination, we performed atomistic molecular dynamics (MD) simulations in explicit solvent of unphosphorylated Ser115 (S115) and phosphorylated Ser115 (p-S115) PIN1 (**Supplementary Fig. S5E; see also Supplementary Methods**). Five independent MD simulations of 100 ns were carried out for each Ser115 state starting from the crystallographic coordinates of PIN1 resolved at 1.35 Å (44). Comparison of the atomic root-mean-square deviations (RMSD) from the starting structure revealed that, although both unphosphorylated and phosphorylated PIN1 displayed low deviations with respect to the X-ray structure, phosphorylated PIN1 showed higher deviations compared to the unphosphorylated PIN1 (**Supplementary Fig. S5F, G**). Consistent with the RMSD results, analyses of the atomic root-mean-square fluctuations (RMSF) revealed a significant increase in the flexibility of residues 115-117 upon phosphorylation of Ser115 (**Supplementary Fig. S5H**). Taken together, our simulations suggest that phosphorylation at Ser115 induces significant local changes in the dynamics of PIN1. Interestingly, analyses of the SASA value for the ten lysine residues of PIN1 throughout the MD simulations revealed a significant decrease in the solvent accessibility of Lys117 upon phosphorylation of Ser115 (**Supplementary Fig. S5I**). All other lysine residues displayed no significant differences in the average SASA values between the unphosphorylated and phosphorylated PIN1 systems (**Fig. 5F**). Representative snapshots from one of the five simulations of phosphorylated PIN1 are shown in **Supplementary Fig. S5J** to illustrate the decrease in the SASA of K117 (from 165 Å to 68 Å) during the course of the simulation time. These observations suggest that PIN1 phosphorylation at Ser115 may inhibit its mono-ubiquitination by decreasing surface exposure of the Lys117 residue and thus its accessibility for ubiquitination.

PIN1 Ser115 phosphorylation promotes cholangiocarcinoma proliferation

We then examined the biological significance of JNK-mediated PIN1 Ser115 phosphorylation on PIN1 function in ICC cells. ICC cells depleted of endogenous PIN1 were reconstituted with rPIN1 WT, shRNA-resistant PIN1 S115A (rPIN1 S115A) or empty vector (EV), and growth rate and colony forming capacity of ICC cells were evaluated. Ectopic expression of rPIN1 WT and rPIN1 S115A was verified by WB (**Fig. 6A**). Of note, rPIN1 WT and rPIN1 S115A had comparable cellular levels that were similar to those of endogenous PIN1 in parental cells (**Fig. 6A**; top panel). In parallel, Phos-tag WB analyses further confirmed that S115A mutation abolishes JNK-mediated phosphorylation signal in ICC cells (**Fig. 6A; see also Fig. 4C**). Reconstitution with rPIN1 S115A, but not rPIN1 WT, failed to rescue the impaired growth rate and ability to grow colonies of PIN1-depleted cells (**Fig. 6B, C**). Moreover, expression of key positive cell-cycle regulators and transcriptional activity of NF-κB (a well-established PIN1 target and ICC cell growth marker) (20,45) were restored by reconstituted expression of rPIN1 WT but not by that of rPIN1 S115A mutant (**Fig. 6A, D**). Thus, phosphorylation of PIN1 at Ser115 by active JNK is critical for promoting ICC cell proliferation.

Pharmacological inhibition of PIN1 impairs cholangiocarcinoma growth

The prolific role of PIN1 in cancer has triggered extensive efforts to design small molecule inhibitors targeting PIN1 function (19-24,36). One such potent inhibitor of PIN1 is ATRA, which binds to PIN1 and induces its degradation (27,36). As the JNK-PIN1 regulatory axis sustains ICC cell proliferation, we explored whether ATRA-induced PIN1 degradation could be used as a therapeutic strategy in cholangiocarcinoma. First, we treated ICC cells with increasing concentrations of ATRA and observed that ATRA treatment resulted in a dose-dependent decrease in the growth rate of ICC cells; yet, ATRA had no effect on nontumoral H69 cholangiocytes (**Fig. 7A**). As expected**,** the decrease in the cell growth rate was associated with a dose-dependent decrease in PIN1 protein levels (**Fig. 7B**), confirming that ATRA prevents PIN1 accumulation in ICC cells. Notably, ATRA treatment did not affect the phosphorylation/activity levels of JNK (**Fig. 7B**). A dose-dependent growth inhibitory effect of ATRA was also observed in ICC cells ectopically expressing PIN1 (**Fig. 7C**). Next, we subcutaneously injected CCLP1 cells into NOD/SCID immunodeficient mice, and two weeks later we implanted either ATRA-releasing pellets or placebo pellets into the flanks of mice to assess the effects of ATRA on the ability of ICC cells to form tumours *in vivo* (**Supplementary Fig S6A**). After a median tumour growth period of 26 days, smaller tumours developed in ATRA-treated group compared with those in placebo-treated mice, as revealed by measuring tumour mass and tumour weight (**Fig. 7D-F; Supplementary Fig. S6B**). WB analyses showed that PIN1 levels markedly decreased in the ATRA-treated tumours compared with those in placebo-treated tumours (**Supplementary Fig.**

S6C). Notably, expression levels of PIN1 did not correlate with those of p-JNK in tumours from ATRA-treated mice (**Supplementary Fig. S6C**; **see also Fig. 7B**), suggesting a potential disruption of JNK-PIN1 regulatory axis by ATRA. These results suggest that ATRA-induced PIN1 degradation may have therapeutic potential against cholangiocarcinoma growth. Last, we examined the biological importance of JNK-mediated PIN1 Ser115 phosphorylation in the response of ICC cells to ATRA. Compared with PIN1-depleted ICC cells reconstituted with rPIN1 WT, PIN1-depleted ICC cells reconstituted with rPIN1 S115A mutant were much less sensitive to ATRA-induced growth inhibition (**Fig. 7G**), implying that PIN1 Ser115 phosphorylation is crucial for the susceptibility of ICC cells towards ATRA.

DISCUSSION

Activation of the JNK signalling pathway in cholangiocytes is a key event in cholangiocarcinogenesis and a promising target in ICC therapy (8). However, due to its multifunctional role in liver homeostasis (12-15), the development of selective therapies that target JNK directly are unlikely to result in clinically translatable options (9,40,46). Therefore, understanding the mechanism through which JNK activation promotes ICC growth and the identification of downstream effectors as druggable targets are a critical step for expanding the therapeutic management of ICC. Here we uncover a mechanistic link between JNK activity and ICC cell proliferation via PIN1 protein stabilization and demonstrate the potential application of the PIN1 inhibitor ATRA for ICC therapy.

Elevated levels of PIN1 were found in ICC cell lines as well as ICC tissues, and positively correlated with the phosphorylation/activity levels of JNK proteins. Intriguingly, the positive association between JNK activity and PIN1 levels appears to be specific to ICC cells as it was not observed in nontumoral human biliary epithelial cells, in which JNK kinase activities are not constitutively upregulated. While blocking JNK activity led to a significant decrease in PIN1 protein levels, ectopic expression of constitutively active form of JNK1 ($JNK1^{CA}$) led to an increase in endogenous PIN1 protein levels. Thus, PIN1 functions downstream of the JNK pathway, consistent with the established role of PIN1 in RAS signalling (16,17,20).

PIN1 was first identified as a key regulator of cell division and later shown to promote tumorigenesis and tumour progression by inactivating proliferation-restraining factors or activating proliferation-promoting factors (20-24). Consistent with the latter, we found that PIN1 is essential for proliferation of both cultured and xenografted ICC cells and functionally mimics JNK activation, thus reflecting the regulatory role of JNK activation on PIN1.

What then is the mechanism by which JNK activity regulates PIN1 expression? Activated JNK proteins regulate a variety of cellular processes, including proliferation, by acting on a number of nuclear and nonnuclear proteins at either transcriptional or posttranslational levels (9,40). We found that JNK activity regulates the intracellular PIN1 levels by stabilizing PIN1 through its phosphorylation, thus preventing PIN1 mono-ubiquitination and proteasomal degradation. This is demonstrated by showing that the newly synthesized endogenous PIN1 displayed a shortened half-life in JNK-depleted or SP600125-treated ICC cells and the decreased intracellular protein levels of PIN1 were reversed by the addition of the proteasome inhibitor MG132. In JNK-depleted ICC cells the decrease in PIN1 levels was associated with the appearance of a mono-ubiquitinated form of PIN1, implying that JNK proteins inhibit the mono-ubiquitination of endogenous PIN1. Furthermore, JNK kinase activity is strictly required for such inhibition as overexpression of the constitutively active form of JNK1, but not its non-active form, inhibited PIN1 mono-ubiquitination. Thus, in accordance with previous works showing that protein stability of PIN1 is regulated through the ubiquitin-proteasome system (34-36) and that small proteins are more likely to be mono-ubiquitinated rather than polyubiquitinated for degradation (37,47), constitutive JNK activation prevents PIN1 mono-ubiquitination-induced proteasomal degradation resulting in the stabilization and elevated levels of PIN1. In line with our finding that JNK activity is required for preventing PIN1 mono-ubiquitination, we show that JNK proteins directly interact with and phosphorylate PIN1 at Ser115, thus pinpointing PIN1 as a direct downstream target of JNK signalling. Moreover, we show that the reconstituted expression of non-phosphorylatable PIN1 S115A mutant, which was resistant to JNK-mediated suppression of PIN1 mono-ubiquitination, failed to revert impaired ICC cell growth. Therefore, the stabilization of PIN1 upon phosphorylation at Ser115 by active JNK represents a causal link between JNK activation and high PIN1 levels and defines the JNK-PIN1 axis as essential for cholangiocarcinoma proliferation. Given that PIN1 is aberrantly expressed at high levels in various types of tumour, including hepatocellular carcinoma, B-cell lymphoma, brain and lung cancer, in which constitutive JNK activation is commonly observed (9,20,36), we speculate that the JNK-mediated stabilization of PIN1 may similarly contribute to the high expression of PIN1 in tumours of diverse tissue origin. Notably, many downstream effectors of the JNK pathway, such as c-Jun and cyclin D1, that promote cancer cell proliferation are reported to be also regulated by PIN1 (9,17,20). Interestingly, we found that the reconstituted expression of PIN1(S115A) mutant but not that of rPIN1 WT failed to revert the levels/activities of key cell proliferation regulators in ICC cells. Thus, it is reasonable to hypothesize that JNK-mediated PIN1 Ser115 phosphorylation may significantly contribute to the pro-proliferative function of activated JNK in many human cancers.

Targeting downstream effectors in JNK signalling is a promising approach for inhibition of tumour proliferation in JNK-dependent tumours (9,40,46). Our results point to PIN1 as a key downstream effector of the JNK pathway and show that the PIN1 inhibitor ATRA (36) effectively impaired ICC cell growth both in *in-vitro* and xenograft experiments with a corresponding decrease in PIN1 levels but not in JNK phosphorylation/activity. Although we cannot rule out that other mechanisms of action of ATRA (21,27) could also be responsible for its growth inhibitory effect in ICC cells, ATRA treatment in ICC cells phenocopies the effects of PIN1 knockdown. Thus, one would expect that ATRA may interfere with the JNK-PIN1 regulatory axis and block its oncogenic function in ICC while leaving JNK activation unaffected.

The obvious question that remains to be addressed is how JNK-mediated Ser115 phosphorylation inhibits PIN1mono-ubiquitination. In agreement with the notion that protein ubiquitination occurs mainly on highly solvent-exposed lysine residues (42,43), we show that the Lys117 of PIN1 is the mono-ubiquitination site targeted for proteasomal degradation. Molecular dynamics simulations suggest that Lys117 displays a decreased solvent accessibility upon phosphorylation at Ser115. Therefore, it is likely that JNK-mediated Ser115 phosphorylation may shield Lys117 from intermolecular interactions with components of the ubiquitination machinery by decreasing its surface exposure. Future investigations are warranted to address this question. Our findings provide insights into the mechanisms by which constitutive JNK activation promotes cholangiocarcinoma growth and identify PIN1 as a direct downstream target of JNK, revealing an unexpected regulatory axis sustaining elevated PIN1 intracellular levels required for cell proliferation (**Fig. 7H**). We propose that targeting PIN1 using ATRA could be a potential therapeutic strategy for ICC. Rapid application of this strategy would be possible as ATRA is an FDA-approved drug to treat APL (27) and is currently being clinically trialled for treatment of other solid cancers (ClinicalTrials.gov: NCT04113863).

REFERENCES

1. Razumilava N, Gores GJ. Cholangiocarcinoma. Lancet. 2014;383:2168-2179.
2. Khan SA, Thomas HC, Davidson BR, Taylor-Robinson SD. Cholangiocarcinoma. Lancet. 2005;366:1303-1314.
3. Guest RV, Boulter L, Dwyer BJ, Forbes SJ. Understanding liver regeneration to bring new insights to the mechanisms driving cholangiocarcinoma. NPJ Regen Med. 2017;2:13.

4. **Zou S, Li J, Zhou H, Frech C, Jiang X, Chu JS**, et al. Mutational landscape of intrahepatic cholangiocarcinoma. Nat Commun. 2014;5:5696.

5. **Ikenoue T, Terakado Y**, Nakagawa H, Hikiba Y, Fujii T, Matsubara D, et al. A novel mouse model of intrahepatic cholangiocarcinoma induced by liver-specific Kras activation and Pten deletion. Sci Rep. 2016;6:23899.

6. Robertson S, Hyder O, Dodson R, Nayar SK, Poling J, Beierl K, et al. The frequency of KRAS and BRAF mutations in intrahepatic cholangiocarcinomas and their correlation with clinical outcome. Hum Pathol. 2013;44:2768-2773.

7. Tannapfel A, Benicke M, Katalinic A, Uhlmann D, Köckerling F, Hauss J, et al. Frequency of p16(INK4A) alterations and K-ras mutations in intrahepatic cholangiocarcinoma of the liver. Gut. 2000;47:721-727.

8. Yuan D, Huang S, Berger E, Liu L, Gross N, Heinzmann F, et al. Kupffer cell-derived Tnf triggers cholangiocellular tumorigenesis through JNK due to chronic mitochondrial dysfunction and ROS. Cancer Cell. 2017;31:771-789.

9. Bubici C, Papa S. JNK signalling in cancer: in need of new, smarter therapeutic targets. Br J Pharmacol. 2014;171:24-37.

10. **Cellurale C, Sabio G**, Kennedy NJ, Das M, Barlow M, Sandy P, et al. Requirement of c-Jun NH(2)-terminal kinase for Ras-initiated tumor formation. Mol Cell Biol. 2011;31:1565-1576.

11. Nielsen C, Thastrup J, Bøttzauw T, Jäättelä M, Kallunki T. c-Jun NH2-terminal kinase 2 is required for Ras transformation independently of activator protein 1. Cancer Res. 2007;67:178-185.

12. Seki E, Brenner DA, Karin M. A liver full of JNK: signaling in regulation of cell function and disease pathogenesis, and clinical approaches. Gastroenterology. 2012;143:307-320.

13. Solinas G, Becattini B. JNK at the crossroad of obesity, insulin resistance, and cell stress response. Mol Metab. 2016;6:174-184.

14. **Cubero FJ, Mohamed MR**, Woitok MM, Zhao G, Hatting M, Nevzorova YA, et al. Loss of c-Jun N-terminal Kinase 1 and 2 function in liver epithelial cells triggers biliary hyperproliferation resembling cholangiocarcinoma. Hepatol Commun. 2020;4:834-851.

15. Manieri E, Folgueira C, Rodríguez ME, Leiva-Vega L, Esteban-Lafuente L, Chen C, et al. JNK-mediated disruption of bile acid homeostasis promotes intrahepatic cholangiocarcinoma. Proc Natl Acad Sci USA. 2020;117:16492-16499.

16. Ryo A, Liou YC, Wulf G, Nakamura M, Lee SW, Lu KP. PIN1 is an E2F target gene essential for Neu/Ras-induced transformation of mammary epithelial cells. Mol Cell Biol. 2002;22:5281-5295.

17. Wulf GM, Ryo A, Wulf GG, Lee SW, Niu T, Petkova V, et al. Pin1 is overexpressed in breast cancer and cooperates with Ras signaling in increasing the transcriptional activity of c-Jun towards cyclin D1. EMBO J. 2001;20:3459-3472.

18. Wulf G, Garg P, Liou YC, Iglehart D, Lu KP. Modeling breast cancer in vivo and ex vivo reveals an essential role of Pin1 in tumorigenesis. EMBO J. 2004;23:3397-3407.

19. Lu KP, Hanes SD, Hunter T. A human peptidyl-prolyl isomerase essential for regulation of mitosis. Nature. 1996;380:544-547.

20. Zhou XZ, Lu KP. The isomerase PIN1 controls numerous cancer-driving pathways and is a unique drug target. Nat Rev Cancer. 2016;16:463-478.

21. Pinch BJ, **Doctor ZM, Nabet B**, Browne CM, Seo HS, Mohardt ML, et al. Identification of a potent and selective covalent Pin1 inhibitor. Nat Chem Biol. 2020;16:979-987.

22. Chen Y, Wu YR, Yang HY, Li XZ, Jie MM, Hu CJ, et al. Prolyl isomerase Pin1: a promoter of cancer and a target for therapy. Cell Death Dis. 2018;9:883.

23. Pu W, Zheng Y, Peng Y. Prolyl isomerase Pin1 in human cancer: function, mechanism, and significance. Front Cell Dev Biol. 2020;8:168.

24. Rustighi A, Zannini A, Campaner E, Ciani Y, Piazza S, Del Sal G. PIN1 in breast development and cancer: a clinical perspective. Cell Death Differ. 2017;24:200-211.

25. **Jhaveri K, Teplinsky E,** Silvera D, Valeta-Magara A, Arju R, Giashuddin S, et al. Hyperactivated mTOR and JAK2/STAT3 Pathways: Molecular Drivers and Potential

Therapeutic Targets of Inflammatory and Invasive Ductal Breast Cancers After Neoadjuvant Chemotherapy. Clin Breast Cancer. 2016; 6:113-22.e1.

26. Gomez-Chou SB, Swidnicka-Siergiejko AK, Badi N, Chavez-Tomar M, Lesinski GB, Bekaii-Saab T, et al. Lipocalin-2 promotes pancreatic ductal adenocarcinoma by regulating inflammation in the tumor microenvironment. Cancer Res. 2017;77:2647-2660.

27. Masetti R, Vendemini F, Zama D, Biagi C, Gasperini P, Pession A. All-trans retinoic acid in the treatment of pediatric acute promyelocytic leukemia. Expert Rev Anticancer Ther. 2012;12:1191-1204.

28. **Tong Y, Ying H,** Liu R, Li L, Bergholz J, Xiao ZX. Pin1 inhibits PP2A-mediated Rb dephosphorylation in regulation of cell cycle and S-phase DNA damage. Cell Death Dis. 2015;6:e1640.

29. Barbarulo A, Iansante V, Chaidos A, Naresh K, Rahemtulla A, Franzoso G, et al. Poly(ADP-ribose) polymerase family member 14 (PARP14) is a novel effector of the JNK2-dependent pro-survival signal in multiple myeloma. Oncogene. 2013;32:4231-4242.

30. Iansante V, Choy PM, Fung SW, Liu Y, Chai JG, Dyson J, et al. PARP14 promotes the Warburg effect in hepatocellular carcinoma by inhibiting JNK1-dependent PKM2 phosphorylation and activation. Nat Commun. 2015;6:7882.

31. Stebbing J, Shah K, Lit LC, Gagliano T, Ditsiou A, Wang T, et al. LMTK3 confers chemo-resistance in breast cancer. Oncogene. 2018;37:3113-3130.

32. Alpini G, Invernizzi P, Gaudio E, Venter J, Kopriva S, Bernuzzi F, et al. Serotonin metabolism is dysregulated in cholangiocarcinoma, which has implications for tumor growth. Cancer Res. 2008;68:9184-9193.

33. Bennett BL, Sasaki DT, Murray BW, O'Leary EC, Sakata ST, Xu W, et al. SP600125, an anthrapyrazolone inhibitor of Jun N-terminal kinase. Proc Natl Acad Sci USA. 2001;98:13681-13686.

34. Eckerdt F, Yuan J, Saxena K, Martin B, Kappel S, Lindenau C, et al. Polo-like kinase 1-mediated phosphorylation stabilizes Pin1 by inhibiting its ubiquitination in human cells. J Biol Chem. 2005;280:36575-36583.

35. Basu A, Das M, Qanungo S, Fan XJ, DuBois G, Haldar S. Proteasomal degradation of human peptidyl prolyl isomerase pin1-pointing phospho Bcl2 toward dephosphorylation. Neoplasia. 2002;4:218-227.

36. Wei S, Kozono S, Kats L, Nechama M, Li W, Guarnerio J, et al. Active Pin1 is a key target of all-trans retinoic acid in acute promyelocytic leukemia and breast cancer. Nat Med. 2015;21:457-466.

37. Swatek KN, Komander D. Ubiquitin modifications. Cell Res. 2016;26:399-422.

38. Yuniati L, Lauriola A, Gerritsen M, Abreu S, Ni E, Tesoriero C, et al. Ubiquitylation of the ER-shaping protein Lunapark via the CRL3KLHL12 ubiquitin ligase complex. Cell Rep. 2020;31:107664.

39. Kinoshita E, Kinoshita-Kikuta E, Koike T. Separation and detection of large phosphoproteins using Phos-tag SDS-PAGE. Nat Protoc. 2009;4:1513-1521.

40. Zeke A, Misheva M, Reményi A, Bogoyevitch MA. JNK Signaling: Regulation and Functions Based on Complex Protein-Protein Partnerships. Microbiol Mol Biol Rev. 2016;80:793-835.

41. Rangasamy V, Mishra R, Sondarva G, Das S, Lee TH, Bakowska JC, et al. Mixed-lineage kinase 3 phosphorylates prolyl-isomerase Pin1 to regulate its nuclear translocation and cellular function. Proc Natl Acad Sci USA. 2012;109:8149-8154.

42. Zhou Y, Liu S, Song J, Zhang Z. Structural propensities of human ubiquitination sites: accessibility, centrality and local conformation. PLoS One. 2013;8:e83167.

43. Catic A, Collins C, Church GM, Ploegh HL. Preferred in vivo ubiquitination sites. Bioinformatics. 2004;20:3302-3307.

44. Ranganathan R, Lu KP, Hunter T, Noel JP. Structural and functional analysis of the mitotic rotamase Pin1 suggests substrate recognition is phosphorylation dependent. Cell. 1997;89:875-886.

45. Yin DL, Liang YJ, Zheng TS, Song RP, Wang JB, Sun BS, et al. EF24 inhibits tumor growth and metastasis via suppressing NF-kappaB dependent pathways in human cholangiocarcinoma. Sci Rep. 2016;6:32167.

46. Messoussi A, Feneyrolles C, Bros A, Deroide A, Daydé-Cazals B, Chevé G, et al. Recent progress in the design, study, and development of c-Jun N-terminal kinase inhibitors as anticancer agents. Chem Biol. 2014;21:1433-1443.

47. **Shabek N, Herman-Bachinsky Y,** Buchsbaum S, Lewinson O, Haj-Yahya M, Hejjaoui M, et al. The size of the proteasomal substrate determines whether its degradation will be mediated by mono- or polyubiquitylation. Mol Cell. 2012;48:87-97.

FIGURE LEGENDS

Figure 1. Active JNK positively correlates and regulates PIN1 levels in human intrahepatic cholangiocarcinoma (ICC). (**A**) Immunohistochemistry on serial sections of 42 paired nontumour adjacent (left panels) and ICC tissue (right panels) stained for phosphorylated JNK (p-JNK) and PIN1. Dot plots graphs indicate the percentage of biliary cells positively stained for p-JNK and PIN1 in nontumour and ICC tissue (n = 42 per group). Data shown in the ICC group are the average results of duplicate samples. Data are presented as mean ± s.e.m, and circles represent individual data points. P value, Wilcoxon matched-pairs signed rank test. Photomicrographs: scale bars 300 μm (top), 100 μm (bottom); magnification 10X (top), 40X (bottom). (**B**) Scatterplots showing the positive correlation between p-JNK and PIN1 protein expression in nontumour adjacent and ICC tissue. Pearson's coefficient tests were performed to assess statistical significance. (**C**) Western blots (WBs) analyses detecting p-JNK and PIN1 in lysates of normal human primary cholangiocytes (HIBEpiC) and ICC-derived cell lines (CCLP1, HuCCT1 and SG231). Actin and total JNK were used as loading control. The arrows denote the expression levels of spliced variants p46 and p54 of JNK1 and JNK2. (**D**) WBs and kinase assay (K.A.) analyses detecting PIN1 expression and JNK1 and JNK2 kinase activities in indicated ICC cell lines and nontumoral human immortalised cholangiocytes (H69) (32). Actin and total JNK1 and JNK2 protein levels were used as loading control. (**E**) WBs showing a reduction of PIN1 levels in indicated ICC cell lines but not in H69 cells infected with lentiviruses expressing JNK1 and JNK2 shRNA (shJNK1/2) compared with control nonspecific (NS) shRNA (shNS). WBs (bottom panels) showing the JNK1/2 knockdown efficiency. The bar graphs represent the quantification of the relative PIN1 levels normalised to actin. (**F**) Bottom, gel of PIN1 mRNA levels, as detected by RT-PCR, in CCLP1-expressing shJNK1/2 and control shNS. Top, graph showing quantification of the data presented as mean ± s.e.m, and circles represent individual

data points. GADPH, control. P value, Student's t-test. (**G**) WBs analyses showing a reduction of PIN1 levels in indicated ICC cell lines treated with 10 μM JNK inhibitor SP600125 compared to vehicle (DMSO)-treated control. Detection of p-JNK, p-c-Jun, p-p38, p-ERK is shown to demonstrate effective inhibition of specific JNK kinase activity. Tubulin, control. The bar graphs represent the quantification of the relative PIN1 levels normalised to tubulin. (**H**) WBs analyses showing increased expression of PIN1 in CCLP1 cells infected with lentiviruses expressing FLAG-tagged constitutive active JNK1 (FLAG-JNK1^{CA}) compared to empty vector (EV). Actin, control. The bar graphs represent the quantification of the relative PIN1 levels normalised to actin. Results are representative of at least three independent experiments.

Figure 2. JNK activity and PIN1 expression are similarly required for ICC cell growth both *in vitro* and *in vivo*. (**A, B**) Growth curves of CCLP1 (n=6), HuCCT1 (n=6), SG231 (n=3) and nontumoral H69 cholangiocytes (n=3) stably expressing PIN1, JNK1/2 or control nonspecific (NS) shRNA (shNS). Data are shown as mean ± s.e.m and are representative of three independent cultures. (**C, D**) Anchorage-independent colony formation of CCLP1 and SG231 cells stably expressing shPIN1, shJNK1/2 or shNS. Representative images show overall view of colony growth after 3 weeks. Data shown are mean ± s.e.m. of three independent cultures, and circles represent individual data points. P values were calculated by Student's t-test. (**E**) WBs showing PIN1 and JNK1/2 protein levels in lysates from CCLP1 cells stable-expressing shNS, shJNK1/2 or shPIN1 used in xenograft experiments (injected cells). Tubulin and total JNK levels were analysed with appropriate antibodies as controls. The bar graphs represent the quantification of the relative PIN1 levels normalised to tubulin. (**F**) Curves of tumour volume plotted over time following inoculation of CCLP1 cells described in (E). P values, two-way ANOVA test. (**G**) Shown are sizes of tumours developed in mice 24 days post-inoculation with CCLP1 cells as described in (E). (**H**) Tumour weight of explanted tumours at day 24 following post-inoculation. P values, one-way ordinary ANOVA test adjusted with Tukey's multiple comparison tests. (**I, K**) Growth curves and anchorage-independent colony formation of CCLP1 ectopically expressing either FLAG-PIN1 (n=3) (I) or FLAG-JNK1^{CA} (n=3) (K) compared to empty vector (EV) (n=3). Shown are representative light microscopy images of cultured cells (days 7 or 8 after cDNA expression) and overall view of colony growth after 3 weeks. Data shown are mean ± s.e.m. of three independent cultures, and circles represent individual data points. P values were calculated by Student's t-test. (**J, L**) WBs showing the ectopic or endogenous (endog.) levels of PIN1 and p-JNK in CCLP1 stably expressing FLAG-PIN1 (J) or FLAG-JNK1^{CA} (L).

Figure 3. Constitutive activation of JNK stabilises PIN1 protein by preventing its mono-ubiquitination and degradation. Results shown are representative of at least three independent experiments. (**A**) Analysis of PIN1 protein stability by pulse-chase experiments in JNK1/2-depleted CCLP1 cells. WBs analyses of PIN1 levels in shJNK1/2- and shNS-expressing CCLP1 cells treated with CHX for the indicated times. Quantification of PIN1 levels relative to tubulin is shown on the right panel. (**B**) WB analyses of PIN1 levels in CCLP1 cells pre-treated with SP600125 (10 μM) for 24 hours followed by CHX treatment for the indicated times. Quantification of PIN1 levels relative to tubulin is shown on the right panel. (**C**) WBs showing PIN1 abundance in JNK1/2-depleted CCLP1 cells treated with either 10 μM MG132 or DMSO (control) for 24 hours. The bar graphs represent the quantification of the relative PIN1 levels normalised to actin. shNS-expressing CCLP1 cells are used as control. (**D**) WBs showing PIN1 abundance in CCLP1 treated with SP600125 (10 μM) for 24 hours followed by co-treatment of SP600125 with either 10 μM MG132 or DMSO (control) for an additional 24 hours. The bar graphs represent the quantification of the relative PIN1 levels normalised to actin. Parental CCLP1 cells treated with DMSO alone are used as control. (**E**) *In-vivo* ubiquitination assays showing accumulation of endogenous monoubiquitinated PIN1 in JNK1/2-depleted CCLP1 cells overexpressing His-HA-tagged ubiquitin, in the presence of MG132. Ubiquitinated proteins were pulled down (PD) with Ni-NTA beads and were analysed by WBs using anti-PIN1 antibody. The arrow indicates the monoubiquitinated PIN1 (PIN1-mUb) band.

Figure 4. JNK directly binds to and phosphorylates PIN1 at Ser115. Results shown are representative of at least three independent experiments. (**A**) Constitutive active JNK1 or JNK2 were immunoprecipitated from lysates of HEK293T cells expressing FLAG-tagged JNK1^{CA} or FLAG-JNK2^{CA}, respectively, and assayed for kinase activity (JNK K.A.) using recombinant GST-PIN1 or control GST proteins as substrates in the presence of (^{32}P)-γ-ATP. WB and Coomassie blue staining indicate loading controls in the bottom panels. (**B**) Immunoprecipitation (IP) followed by WBs showing endogenous association of active JNK1 with PIN1 in parental CCLP1 cells. IP against IgG and lysates of PIN1-depleted (shPIN1) CCLP1 cells were used as control. The purple-coloured asterisks indicate PIN1 band present in the anti-PIN1 blot. (**C**) Phos-tag analysis in JNK1/2-depleted or SP600125-treated CCLP1 ICC cells showing reduction of endogenous phospho(p)-PIN1 levels compared to control cells (shNS; DMSO). Tubulin, loading control. (**D**) *In-vitro* JNK kinase assay (K.A.) was performed by incubating recombinant activated JNK1 (Rec. active-JNK1) with His-PIN1 as substrate. [^{32}P]-Rec. active-JNK1 denotes autophosphorylation. Coomassie staining shows the purity and size of the recombinant proteins. (**E**) *In-vitro* pull-down assay showing a direct binding between purified active-JNK1 and PIN1. The assay was

performed by IP and WB after incubating purified rec. active JNK1 and His-PIN1 (IP:JNK1 and WB:PIN1). (**F**) Activated JNK was immunoprecipitated from lysates of HEK293T cells expressing FLAG-tagged JNK1^{CA} and assayed for kinase activity (K.A.) using purified His-tagged PIN1-WT, -S114A, -S115A or -S138A as substrate in the presence of (^{32}P)-γ-ATP. WB against p-JNK and Coomassie staining indicate loading controls. (**G**) Phos-tag analysis of PIN1 S115 phosphorylation by endogenous JNK in CCLP1 cells stably expressing PIN1-WT or the indicated PIN1 mutants. Phosphorylated PIN1 band is absent in CCLP1 cells expressing FLAG-PIN1(S115A) mutant. An aliquot of lysates from CCLP1 cells expressing FLAG-PIN1-WT was treated with calf-intestinal alkaline phosphatase (CIP) before electrophoresis and loaded onto the same gel on a distant lane. All the other samples were incubated at 37°C in the presence of CIP buffer only. (Bottom) Standard WBs were carried on whole-cell lysates using anti-FLAG antibody.

Figure 5. JNK-mediated PIN1 Ser115 phosphorylation prevents its mono-ubiquitination at Lys117. Results shown are representative of at least three independent experiments. (**A**) Analysis of PIN1 wild type (WT) and PIN1 mutant proteins stability by pulse-chase experiments. CCLP1 cells overexpressing FLAG-tagged PIN1-WT or PIN1 mutants (S114A, S115A, S138A) were treated with CHX for the indicated times, harvested and analysed by WBs as indicated. Quantification of FLAG-PIN1 levels relative to tubulin is shown on the right panel. (**B**) *In-vivo* ubiquitination assays showing the level of mono-ubiquitination of PIN1-WT and PIN1-S115A mutant proteins in CCLP1 cells stably co-expressing His-HA-Ubiquitin (Ub) with FLAG-PIN1-WT or FLAG-PIN1-S115A, in the presence of MG132. Ubiquitinated proteins were pulled down (PD) with Ni-NTA beads and analysed by WB using anti-FLAG antibody. (**C**) Ribbon representation of PIN1 color-coded by domain (grey, WW domain; blue, PPIase domain). The 10 lysine residues of the enzyme are shown with ball-and-sticks (green C, blue N and white H atoms) and values in parentheses indicate the relative solvent accessibility of their side-chain atoms (RSA, %), as calculated from a high-resolution crystal structure of PIN1 (PDB ID: 1PIN) using NACCESS. Also shown with orange C atoms are S115, C113 and the catalytic site histidine residues H59 and H157 (O atoms are shown in red and S in yellow). (**D**) *In-vivo* ubiquitination assay in SP600125-treated CCLP1 cells stably co-expressing His-HA-Ubiquitin (Ub) with FLAG-PIN1-WT or FLAG-PIN1-K117R. Left, ubiquitinated proteins were pulled down (PD) with Ni-NTA beads and analysed by WBs using anti-FLAG antibody. Right, immunoprecipitation (IP) with anti-FLAG antibody followed by WBs with anti-Ubiquitin antibody. (**E**) Analysis of PIN1-WT and PIN1-K117R proteins stability by pulse-chase experiments. Following treatment with SP600125, CCLP1 cells overexpressing FLAG-PIN1-WT or FLAG-PIN1-K117R mutant were treated with CHX for the indicated times, harvested and analysed by WB as indicated. Quantification of FLAG-PIN1 levels

relative to tubulin is shown on the right panel. (**F**) Left, plot of the mean solvent accessible surface area (SASA) for each lysine residue of PIN1 (side-chain atoms only), calculated from (n=5) independent 100 ns MD simulations of the enzyme in the unphosphorylated (S115) or phosphorylated (p-S115) state of Ser115. Data in bar graph are presented as mean ± s.e.m, and circles represent individual data points. P values, multiple t-test. Right, volcano plot showing the estimated SASA fold changes between S115 and p-S115 (x-axis) versus the $-\log_{10}$ p-values (y-axis) for each lysine of PIN1. Dotted grid lines are shown at x=0 (no difference) and y=-$\log_{10}(0.05)$. K117 is the only lysine showing a significant difference.

Figure 6. PIN1 Ser115 phosphorylation promotes ICC cell growth. (**A**) Representative of three independent WB showing the effect of PIN1 reconstitution in CCLP1 cells depleted of endogenous PIN1. Cells were reconstituted with cDNA expressing shRNA-resistant FLAG-PIN1 WT (rPIN1 WT), FLAG-PIN1 S115A (rPIN1 S115A) or empty vector (-). Lysates of CCLP1 parental cells (first lane) were used as control for endogenous (endog.) PIN1 expression levels. Shown are Phos-tag and classic WB analyses displaying a correlation of expression between phospho(p)-PIN1 levels and cyclin D1, E and A. Tubulin was used as loading control. (**B**) shPIN1-expressing CCLP1 and SG231 ICC cells were reconstituted with rPIN1 WT, rPIN1 S115A or empty vector (EV) and cell growth was quantified at the indicated times. Data presented as mean ± s.e.m. (**C**) Colony-formation assay was performed in shPIN1-expressing CCLP1 and SG231 cells reconstituted with rPIN1 WT, rPIN1 S115A or EV. Data presented as mean ± s.e.m, and circles represent individual data points. P values, one-way ordinary ANOVA test adjusted with Dunnett's multiple comparison tests. (**D**) Transcriptional activity of NF-kB (left) and STAT3 (right) in shPIN1-expressing CCLP1 cells reconstituted with rPIN1 WT, rPIN1 S115A or EV. Data presented as mean ± s.e.m and circles represent individual data points. P values, one-way ordinary ANOVA test adjusted with Dunnett's multiple comparison tests. a.u., arbitrary units.

Figure 7. PIN1 inhibition by ATRA impairs cholangiocarcinoma growth *in vivo*. (**A**) Cell viability assay of CCLP1, HuCCT1, SG231 ICC cells and nontumoral H69 cholangiocytes treated with ATRA for 72 h and assayed with colorimetric MTT assay. Data are shown as mean ± s.e.m and are the combination of (n=4) independent cultures. P values, two-way ANOVA test. (**B**) WB and quantification analyses showing reduction of PIN1 levels, but not of p-JNK, in CCLP1 and SG231 ICC cell lines following 48 hours treatment with the indicated concentrations of ATRA. Tubulin and total-JNK were used as loading controls. (**C**) Anchorage-independent colony formation of CCLP1 expressing FLAG-PIN1 and treated with the indicated concentrations of ATRA. Representative images show overall view of colony growth after 3 weeks. Data shown are

mean ± s.e.m. of three independent cultures and circles represent individual data points. P values, one-way ordinary ANOVA test adjusted with Dunnett's multiple comparison tests. (**D**) Shown are sizes of tumours developed in nude mice inoculated with CCLP1 cells and, 13 days later, implanted with ATRA-releasing (10 mg over 21 day) or placebo (control) pellets. (**E**) Tumour weight of explanted tumours at day 26 following ATRA or placebo treatment. P value, Student's t-test. (**F**) Curves of tumour volume plotted over time following ATRA or placebo treatment. P values, two-way ANOVA test. (**G**) Cell viability assay of shPIN1-expressing CCLP1 cells reconstituted with rPIN1 WT, rPIN1 S115A or EV and treated with the indicated concentrations of ATRA for 72 hours. Data are shown as mean ± s.e.m and are the combination of three independent cultures. P values, two-way ANOVA test. (**H**) Schematic illustration depicting the mechanism of action of JNK-mediated cholangiocarcinogenesis. In response to growth factors, inflammatory cytokines and oncogenic signals, cancer cells activate the JNK signalling pathway via a phosphorylation (P) cascade that involves oncogenic RAS, MAP3K and MAP2K. Active JNK directly binds and phosphorylates PIN1 at S115. This phosphorylation prevents PIN1 mono-ubiquitination (Ub) at Lys117 (K117) and subsequent proteasomal degradation, contributing to the intracellular accumulation of PIN1 in cancer cells. The targeting of PIN1 with a*ll-trans* retinoic acid (ATRA) uncouples the JNK-PIN1 axis and impairs the JNK-mediated cholangiocarcinogenesis.

Figure 1

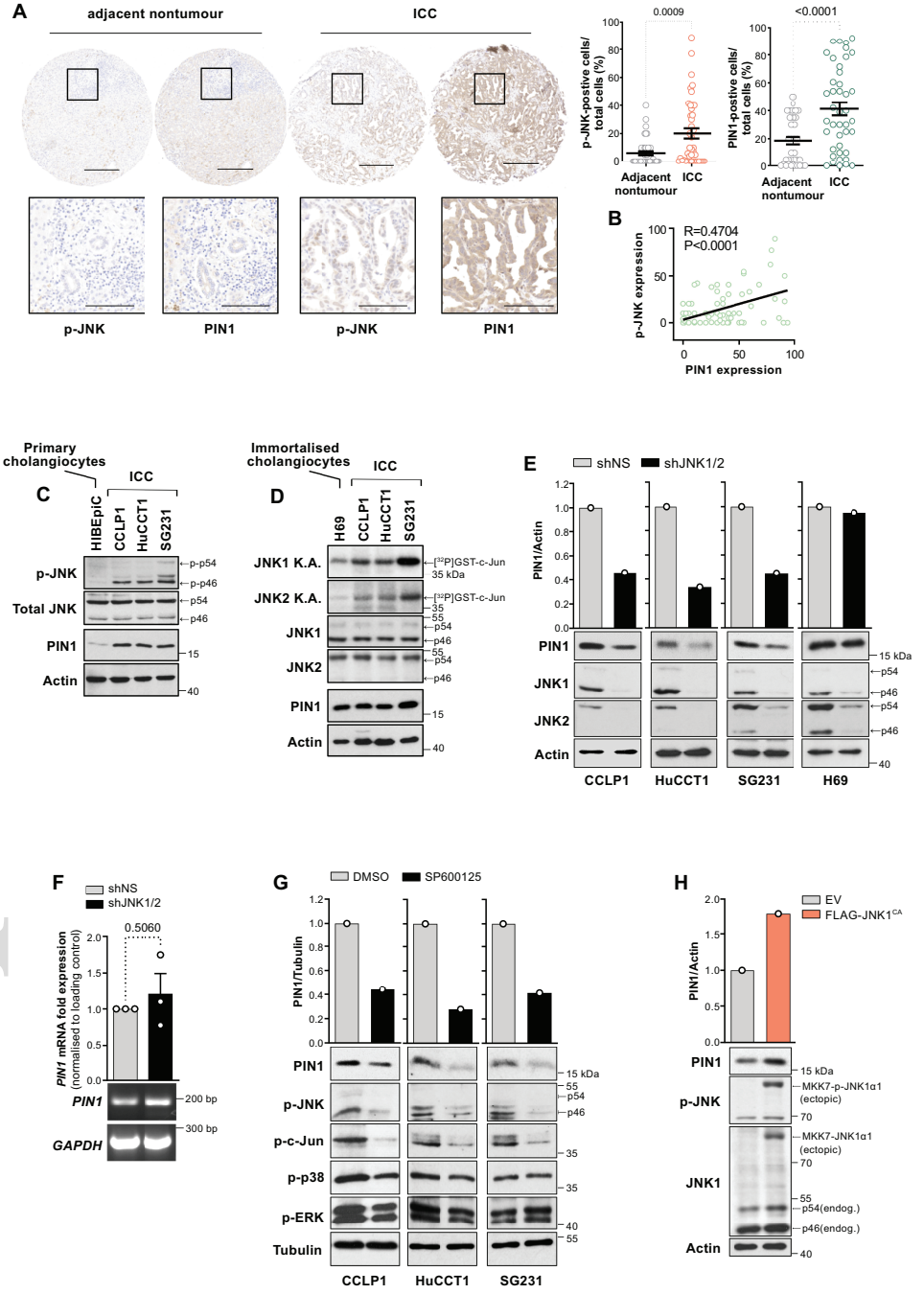

Figure 2

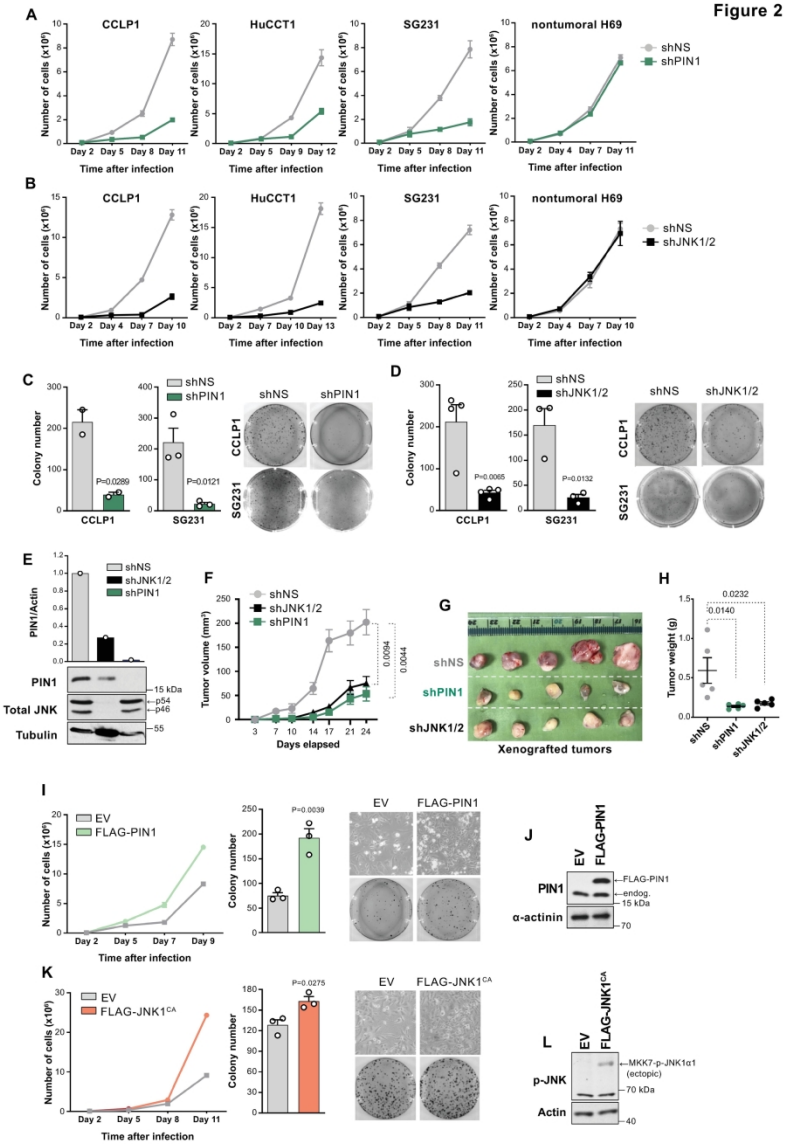
A
CCLP1
HuCCT1
SG231
nontumoral H69
Number of cells (x10⁶)
Time after infection
shNS
shPIN1
B
shNS
shJNK1/2
C
Colony number
P=0.0289
P=0.0121
CCLP1
SG231
D
P=0.0065
P=0.0132
E
PIN1/Actin
PIN1
Total JNK
Tubulin
15 kDa
p54
p46
55
F
Tumor volume (mm³)
Days elapsed
0.0094
0.0044
G
Xenografted tumors
H
Tumor weight (g)
0.0232
0.0140
I
EV
FLAG-PIN1
P=0.0039
J
FLAG-PIN1
endog.
15 kDa
α-actinin
70
K
FLAG-JNK1CA
P=0.0275
L
MKK7-p-JNK1α1
(ectopic)
70 kDa
p-JNK
Actin
40

Figure 3

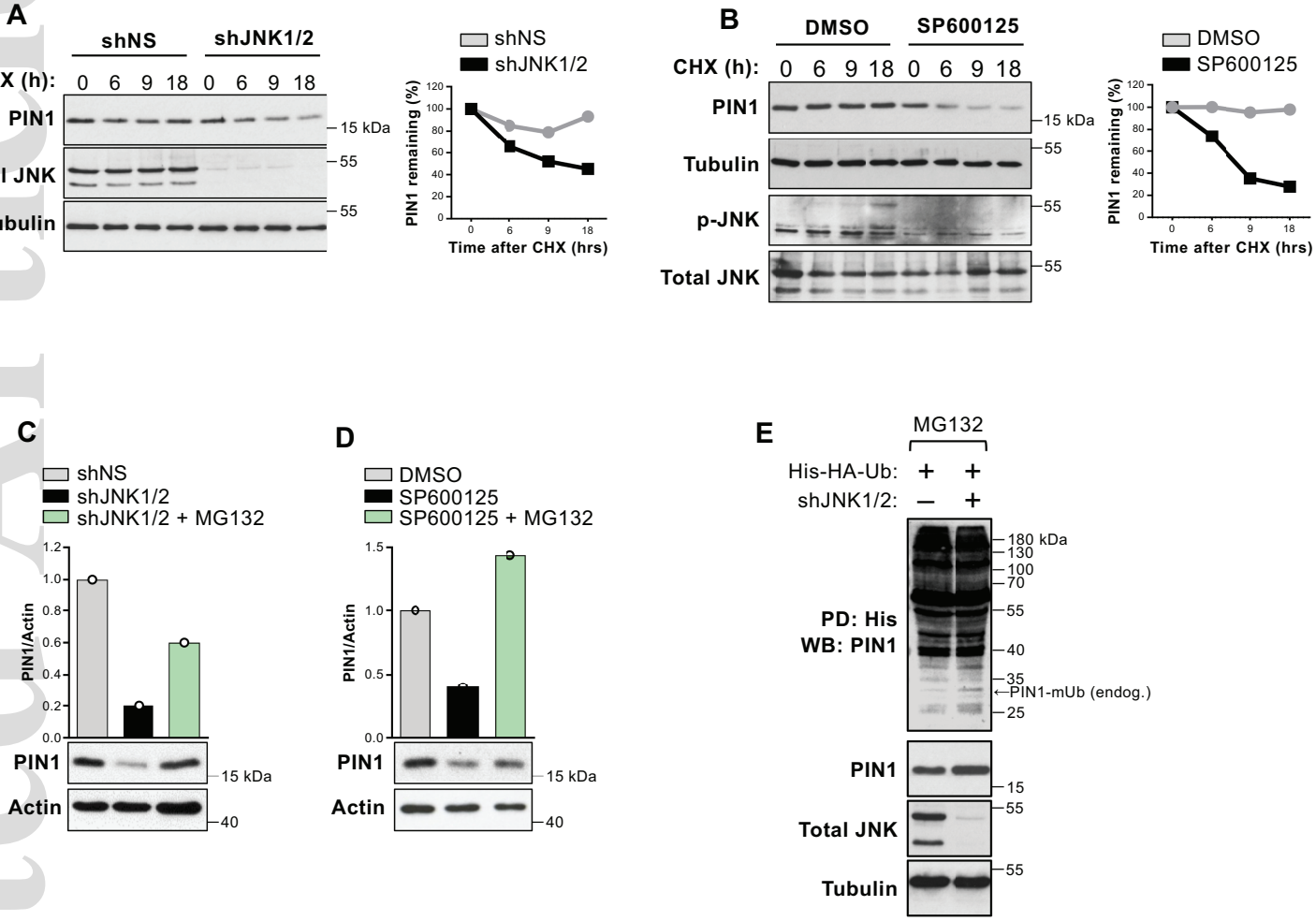

hep_31983_f3.eps

Figure 4

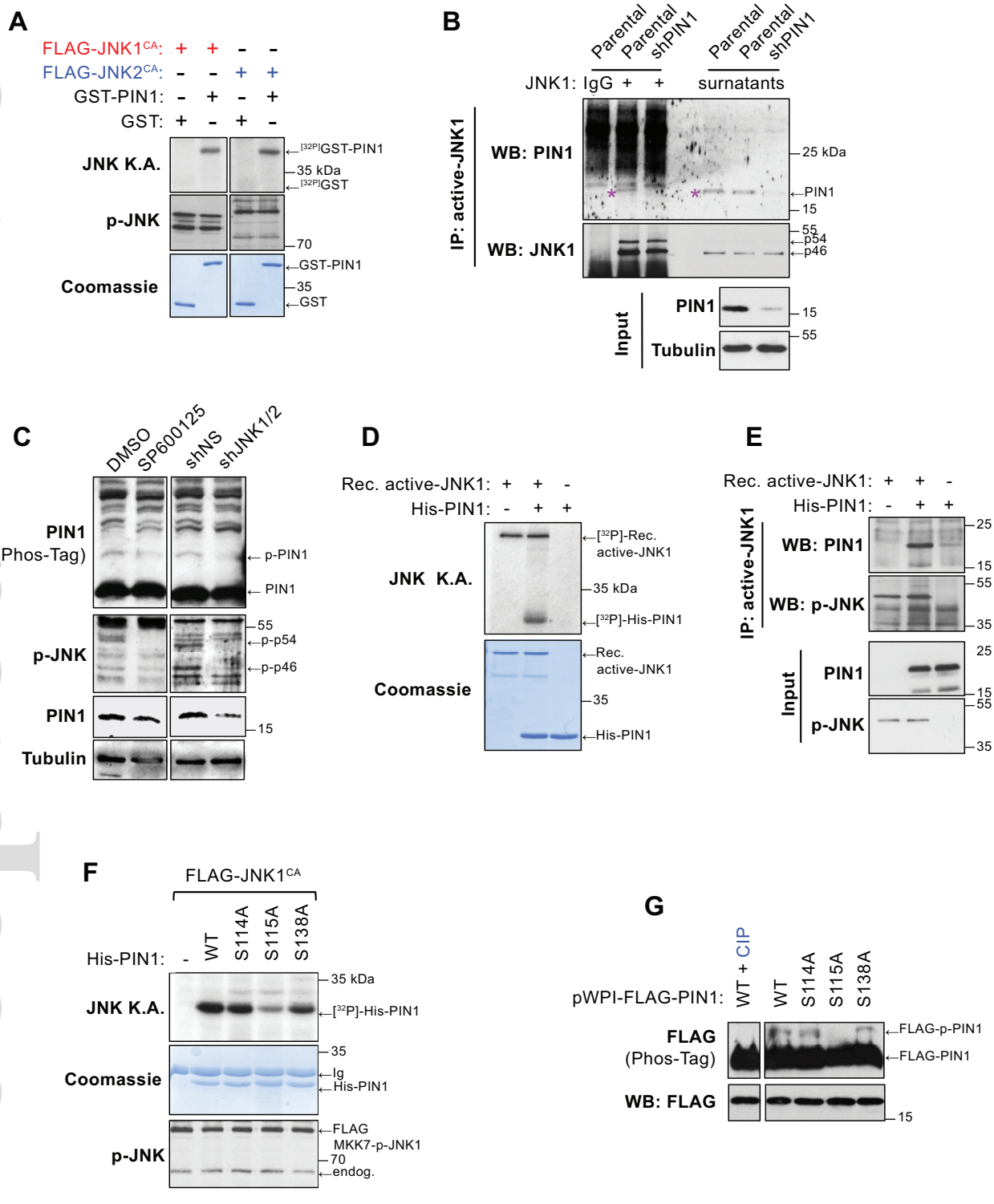

hep_31983_f4.eps

Figure 5

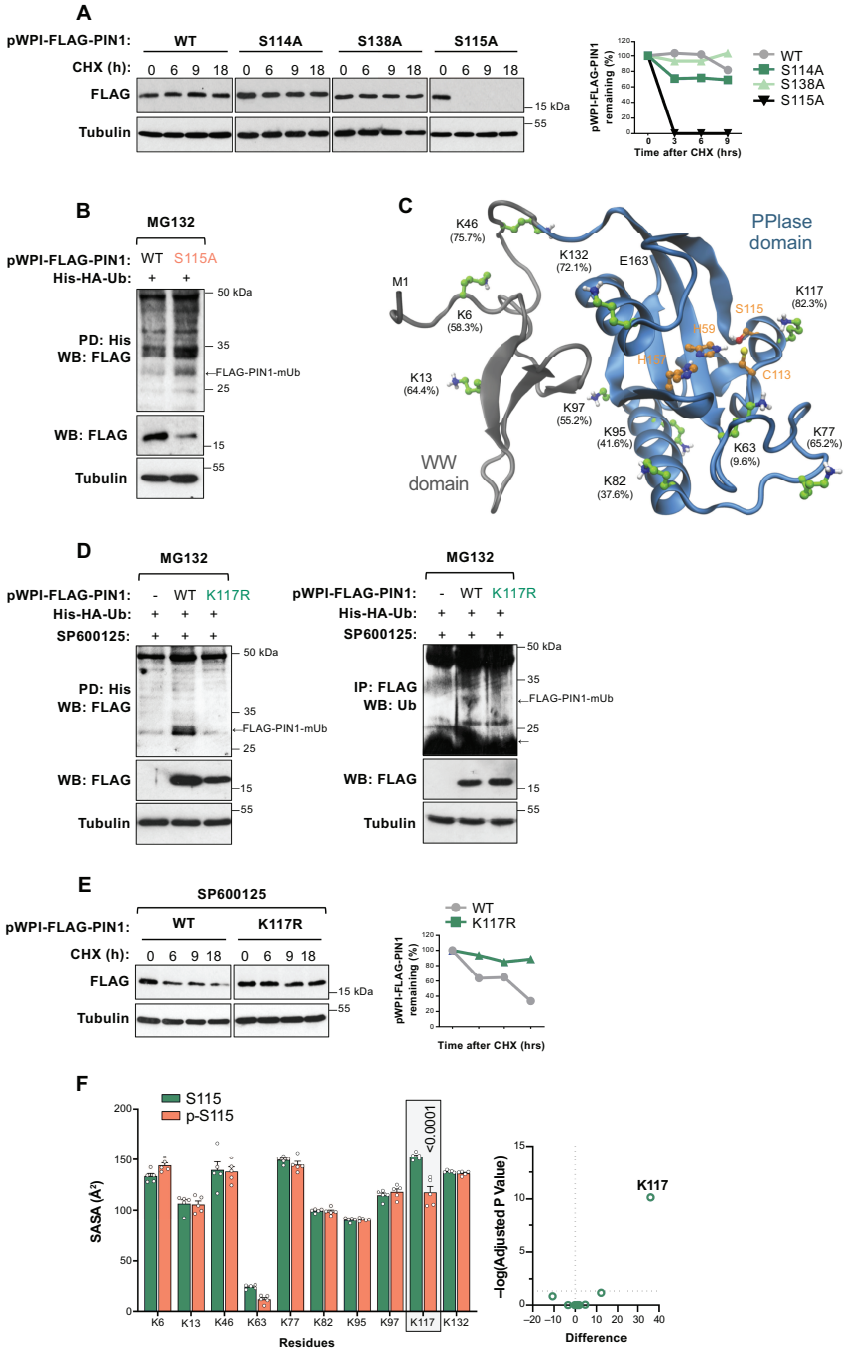

Figure 6

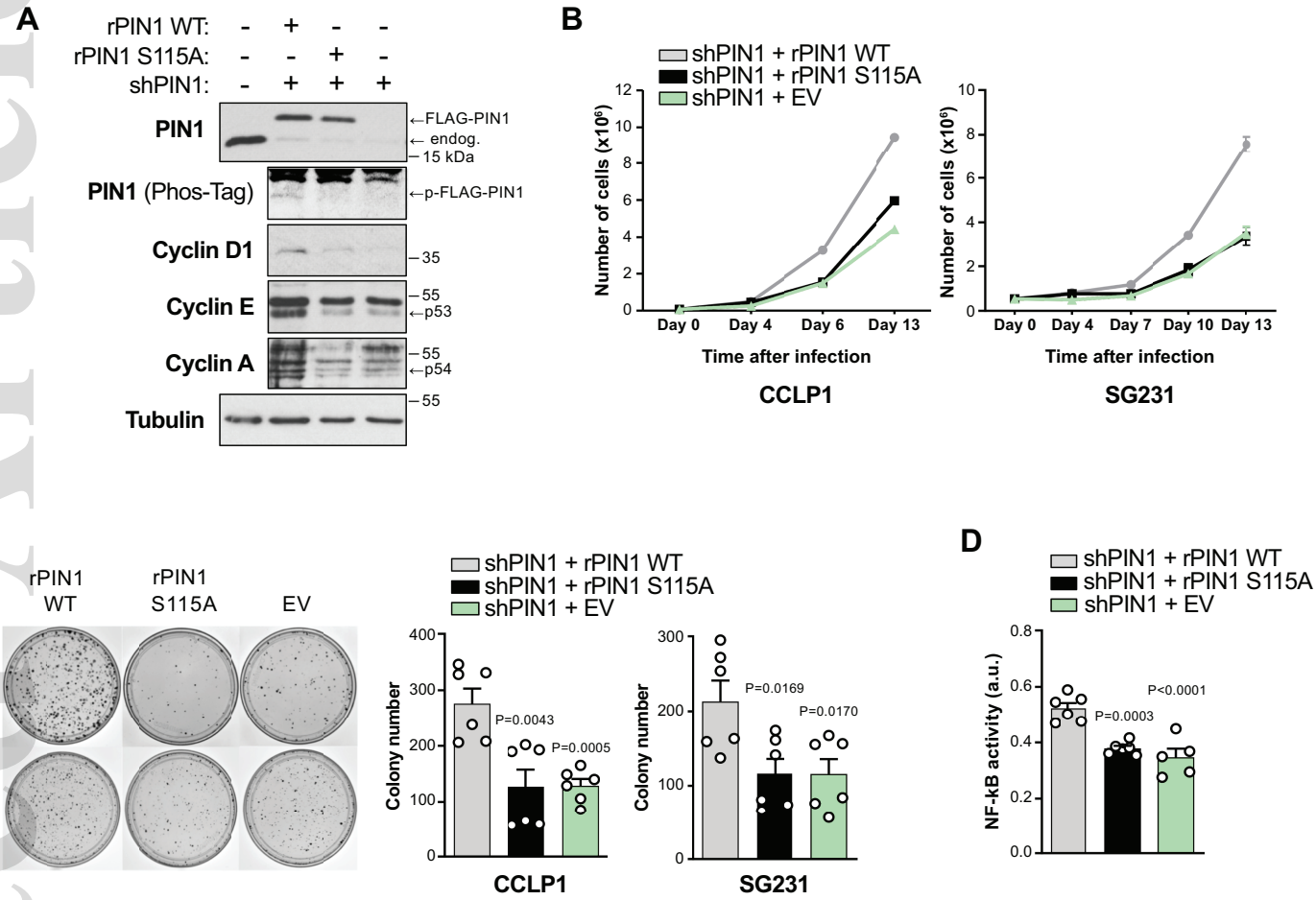

hep_31983_f6.eps

Figure 7